J|A|C|S ARTICLES

Published on Web 12/16/2010

NMR Characterization of a "Fibril-Ready" State of Demetalated Wild-Type Superoxide Dismutase

Lucia Banci,[†,‡] Ivano Bertini,*[,†,‡] Olga Blaževitš,[†] Francesca Cantini,[†,‡] Moreno Lelli,[†,§] Claudio Luchinat,[†,‡] Jiafei Mao,[†] and Miguela Vieru[†]

Magnetic Resonance Center (CERM), University of Florence, Via L. Sacconi 6, 50019 Sesto Fiorentino, Italy, and Department of Chemistry "Ugo Shiff", University of Florence, Via della Lastruccia 3, 50019, Sesto Fiorentino, Italy

Received August 4, 2010; E-mail: ivanobertini@cerm.unifi.it

Abstract: Demetalated superoxide dismutase (SOD1) is a transient species, fibrillogenic in nature and of biomedical interest. It is a conformationally disordered protein difficult to characterize. We have developed a strategy based on the NMR investigation of a crystalline species characterized by X-ray crystallography and on the comparison of the solid-state−solution-state chemical shifts. The solid-state assignment has been also helpful in assigning the solution spectra. The solution NMR spectra presumably detect species that are the result of equilibria among multiple species. From the differences in chemical shifts between the two forms, we learned that a β-sheet becomes conformationally labile and two loops in the same sheet show propensity to take a β conformation. This strategy, which exploits solution and solid-state NMR spectra in a synergistic way, thus provides information on the species that are prone to oligomerize.

Introduction

Cu,Zn-superoxide dismutase (SOD1), a 32 kDa homodimeric superoxide scavenger enzyme, is an indispensable member of the cellular defense system against oxidative stress in the human body. Each of its subunits in the mature form contains one zinc ion, one copper ion, and a conserved intrasubunit disulfide bond between Cys57 and Cys146. Human SOD1 contains also two other cysteine residues (Cys6 and Cys111) per subunit, which are apart from one another and are in the reduced state. The copper ion is essential for the enzymatic dismutase activity, while the zinc ion and the intrasubunit disulfide bond are crucial for maintaining the structural stability of SOD1.[1] SOD1 is a nuclear encoded protein that mainly localizes in the cytoplasm, but it is also present in the peroxisomes, in the mitochondrial intermembrane space (about 10% of the total SOD1), and in the nucleus of eukaryotic cells.[2−4]

SOD1 and in particular its demetalated form are believed to be in some way linked to the familial form of amyotrophic lateral sclerosis (fALS), a fatal motor neurodegenerative disease.[5−9] It gives rise to insoluble protein aggregates of amyloid nature *in vivo* under a number of conditions[10−14] that have not yet been fully elucidated, whereas *in vitro* exposure to air at physiological temperature and pH is enough for the production of soluble oligomers with a molecular organization of amyloid type.[6,15] Therefore the characterization of the demetalated SOD1 protein is relevant for understanding its mode of aggregation.

NMR characterization and gel filtration experiments of the apo state showed that the protein is monomeric when the

† CERM.
‡ Department of Chemistry "Ugo Shiff".
§ Current address: Centre de RMN à Très Hauts Champs, FRE 3008 CNRS/Ecole Normale Supérieure de Lyon, 5 Rue de la Doua, 69100 Villeurbanne, France.

(1) Bertini, I.; Mangani, S.; Viezzoli, M. S. Structure and properties of copper/zinc superoxide dismutases. In *Advanced Inorganic Chemistry*; Sykes, A. G., Ed.; Academic Press: San Diego, CA, USA, 1998; pp 127−250.
(2) Okado-Matsumoto, A.; Fridovich, I. *J. Biol. Chem.* **2001**, *276*, 38388–38393.
(3) Field, L. S.; Furukawa, Y.; O'Halloran, T. V.; Culotta, V. C. *J. Biol. Chem.* **2003**, *278*, 28052–28059.
(4) Sturtz, L. A.; Diekert, K.; Jensen, L. T.; Lill, R.; Culotta, V. C. *J. Biol. Chem.* **2001**, *276*, 38084–38089.
(5) Furukawa, Y.; O'Halloran, T. V. *J. Biol. Chem.* **2005**, *280*, 17266–17274.
(6) Banci, L.; Bertini, I.; Girotto, S.; Martinelli, M.; Vieru, M.; Whitelegge, J.; Durazo, A.; Valentine, J. S. *Proc. Natl. Acad. Sci. U. S. A.* **2007**, *104*, 11263–11267.
(7) Chattopadhyay, M.; Valentine, J. S. *Antioxid. Redox. Signal.* **2009**, *11*, 1603–1614.
(8) Lindberg, M. J.; Tibell, L.; Oliveberg, M. *Proc. Natl. Acad. Sci. U. S. A.* **2002**, *99*, 16607–16612.
(9) Cozzolino, M.; Pesaresi, M. G.; Amori, I.; Crosio, C.; Ferri, A.; Nencini, M.; Carri, M. T. *Antioxid. Redox. Signal.* **2009**, *11*, 1547–1558.
(10) Wang, J.; Xu, G.; Borchelt, D. R. *J. Neurochem.* **2006**, *96*, 1277–1288.
(11) Jonsson, P. A.; Ernhill, K.; Andersen, P. M.; Bergemalm, D.; Brannstrom, T.; Gredal, O.; Nilsson, P.; Marklund, S. L. *Brain* **2004**, *127*, 73–88.
(12) Deng, H. X.; Shi, Y.; Furukawa, Y.; Zhai, H.; Fu, R.; Liu, E.; Gorrie, G. H.; Khan, M. S.; Hung, W. Y.; Bigio, E. H.; Lukas, T.; Dal Canto, M. C.; O'Halloran, T. V.; Siddique, T. *Proc. Natl. Acad. Sci. U. S. A.* **2006**, *103*, 7142–7147.
(13) Johnston, J. A.; Dalton, M. J.; Gurney, M. E.; Kopito, R. R. *Proc. Natl. Acad. Sci. U. S. A.* **2000**, *97*, 12571–12576.
(14) Furukawa, Y.; Fu, R.; Deng, H. X.; Siddique, T.; O'Halloran, T. V. *Proc. Natl. Acad. Sci. U. S. A.* **2006**, *103*, 7148–7153.
(15) Banci, L.; Bertini, I.; Boca, M.; Girotto, S.; Martinelli, M.; Valentine, J. S.; Vieru, M. *Plos ONE* **2008**, *3*, e1677.

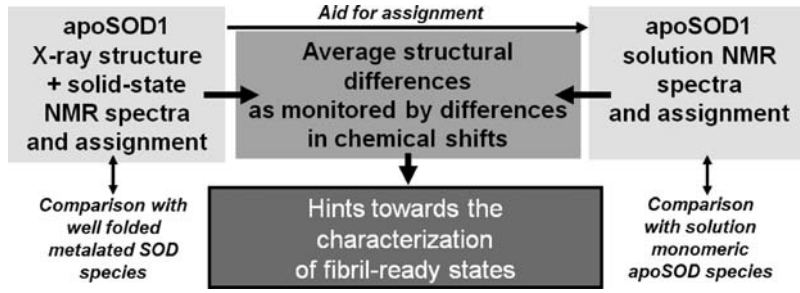

Figure 1. Schematic outline of the approach used in this work.

intrasubunit disulfide bond is reduced.[16−18] Moreover the reduced apo monomeric form is in a molten globule state,[8,19] and this property is considered necessary for SOD1 import in the mitochondrial IMS.[3] Oxidation of Cys57 and Cys146 leads to dimer formation, *in vitro* and possibly in the IMS.[16] There is a general belief that the apo form is the species that undergoes protein oligomerization *in vitro*.[6,10,20−23] For this reason we attempted its characterization by NMR in solution.[19] The protein was found to be highly mobile and disordered. Many NMR signals are not detected due to conformational exchange processes. The signal dispersion is poor, and no long-range NOEs could be observed. Therefore only limited structural information could be obtained. However, crystals of the apo state of wild-type SOD1 (apo wtSOD1) were obtained at 288 K and showed a reasonably structured protein,[19] similar to all X-ray structures of various SOD1 forms.[24−26] This was apparently a consequence of the crystallization process that favors one of the conformations among the many adopted by the apo form in solution.[19]

Here we report a deeper characterization of the demetalated species in solution through a strategy that combines solid-state and solution NMR data. By assigning the solid-state NMR spectra and analyzing the chemical shift differences with the solution spectra (Figure 1), we were able to highlight the parts of the sequence that are more prone to—and could therefore initiate—fibril formation.

Materials and Methods

Protein Preparation. Uniformly [^{13}C,^{15}N]-labeled Cu,Zn wt-SOD1 and Cu,Zn ASSOD1 were expressed and purified as described before.[19] In the latter construct two mutations were introduced at free Cys6 and Cys111 (C6A and C111S). This is a more thermostable form with respect to degradation, as previously found in solution.[27,28] The proteins were then demetalated following published protocols.[29] Samples of apo wtSOD1 in solution reached around 0.6 mM protein concentration in 50 mM phosphate at pH 7.

Microcrystals of apo wtSOD1 and apo ASSOD1 were obtained by 3 weeks' vapor diffusion at 288 K from 0.1 mM protein solutions (0.1 M Mes, 30% PEG 3350, pH 6.0).

NMR Measurements and Analysis. All the solid-state NMR spectra were recorded on a Bruker Avance 850 MHz wide-bore instrument operating at 20.0 T (850 MHz ^{1}H Larmor frequency, 214 MHz ^{13}C Larmor frequency). Solution NMR ^{13}C spectra were acquired on a Bruker Avance 700 MHz spectrometer operating at 16.4 T (176.0 MHz ^{13}C Larmor frequency) and equipped with a ^{1}H and ^{13}C cryoprobe. The effective sample temperature was stabilized at 288 K for all solution and solid-state NMR experiments. Standard sequences were used for the set of SSNMR spectra (2D DARR, 2D NCA, 2D NCO, 3D NCACX, 3D NCOCX).[30−32] The details on the experiments and data processing are reported in the Supporting Information (SI).

The TALOS+ program[33] was used to predict the β or α propensity of each residue using the Cα, Cβ, C′, and N chemical shift values of apo wtSOD1 both in solution and in microcrystals and of the apo monomeric form of SOD (M2 ASSOD[34]) as input.

Results and Discussion

The solid-state NMR ^{13}C−^{13}C DARR (dipolar-assisted rotational resonance) spectrum of apo wtSOD1 microcrystals exhibits a large number of well-resolved cross-peaks (about 1500), although less than the number of peaks observed in the

(16) Arnesano, F.; Banci, L.; Bertini, I.; Martinelli, M.; Furukawa, Y.; O'Halloran, T. V. *J. Biol. Chem.* **2004**, *279*, 47998–48003.
(17) Hörnberg, A.; Logan, D. T.; Marklund, S. L.; Oliveberg, M. *J. Mol. Biol.* **2007**, *365*, 333–342.
(18) Lindberg, M. J.; Normark, J.; Holmgren, A.; Oliveberg, M. *Proc. Natl. Acad. Sci. U. S. A.* **2004**, *101*, 15893–15898.
(19) Banci, L.; Bertini, I.; Boca, M.; Calderone, V.; Cantini, F.; Girotto, S.; Vieru, M. *Proc. Natl. Acad. Sci. U. S. A.* **2009**, *106*, 6980–6985.
(20) Furukawa, Y.; O'Halloran, T. V. *Antioxid. Redox. Signal.* **2006**, *8*, 847–867.
(21) Rakhit, R.; Crow, J. P.; Lepock, J. R.; Kondejewski, L. H.; Cashman, N. R.; Chakrabartty, A. *J. Biol. Chem.* **2004**, *279*, 15499–15504.
(22) Nordlund, A.; Leinartaite, L.; Saraboji, K.; Aisenbrey, C.; Grobner, G.; Zetterstrom, P.; Danielsson, J.; Logan, D. T.; Oliveberg, M. *Proc. Natl. Acad. Sci. U. S. A.* **2009**, *106*, 9667–9672.
(23) Teilum, K.; Smith, M. H.; Schulz, E.; Christensen, L. C.; Solomentsev, G.; Oliveberg, M.; Akke, M. *Proc. Natl. Acad. Sci. U. S. A.* **2009**, *106*, 18273–18278.
(24) Strange, R. W.; Antonyuk, S.; Hough, M. A.; Doucette, P. A.; Rodriguez, J. A.; Hart, P. J.; Hayward, L. J.; Valentine, J. S.; Hasnain, S. S. *J. Mol. Biol.* **2003**, *28*, 877–882.
(25) Hough, M. A.; Grossmann, J. G.; Antonyuk, S. V.; Strange, R. W.; Doucette, P. A.; Rodriguez, J. A.; Whitson, L. J.; Hart, P. J.; Hayward, L. J.; Valentine, J. S.; Hasnain, S. S. *Proc. Natl. Acad. Sci. U. S. A.* **2004**, *101*, 5976–5981.
(26) Elam, J. S.; Taylor, A. B.; Strange, R.; Antonyuk, S.; Doucette, P. A.; Rodriguez, J. A.; Hasnain, S. S.; Hayward, L. J.; Valentine, J. S.; Yeates, T. O.; Hart, P. J. *Nat. Struct. Biol.* **2003**, *10*, 461–467.
(27) Hallewell, R. A.; Imlay, K. C.; Laria, I.; Gallegos, C.; Fong, N. M.; Irvine, B.; Cabelli, D. E.; Bielski, B. H. J.; Olson, P.; Mullenbach, G. T.; Cousens, L. S. *Biochem. Biophys. Res. Commun.* **1991**, *181*, 474–480.
(28) Banci, L.; Cabelli, D. E.; Getzoff, E. D.; Hallewell, R. A.; Viezzoli, M. S. *J. Inorg. Biochem.* **1993**, *50*, 89–100.
(29) McCord, J. M.; Fridovich, I. *J. Biol. Chem.* **1969**, *244*, 6049–6055.
(30) Takegoshi, K.; Nakamura, S.; Terao, T. *Chem. Phys. Lett.* **2001**, *344*, 631–637.
(31) Pauli, J.; Baldus, M.; van Rossum, B.; de Groot, H.; Oschkinat, H. *Chembiochem.* **2001**, *2*, 272–281.
(32) Castellani, F.; van Rossum, B. J.; Diehl, A.; Rehbein, K.; Oschkinat, H. *Biochemistry* **2003**, *42*, 11476–11483.
(33) Shen, Y.; Delaglio, F.; Cornilescu, G.; Bax, A. *J. Biomol. NMR* **2009**, *44*, 213–223.
(34) Banci, L.; Bertini, I.; Cramaro, F.; Del Conte, R.; Viezzoli, M. S. *Biochemistry* **2003**, *42*, 9543–9553.

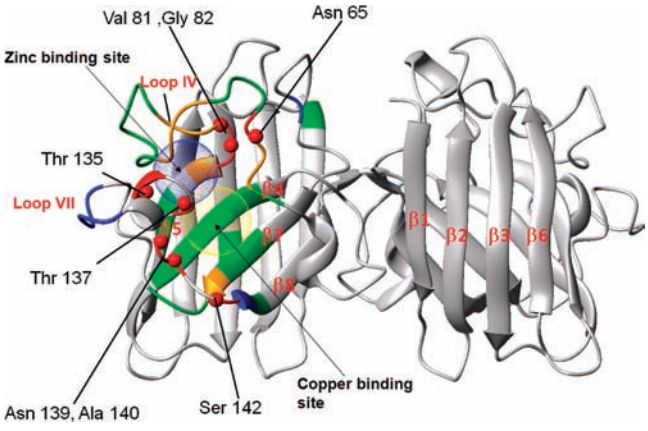

Figure 2. X-ray structure of apo wtSOD1 (PDB code 3ECU). The missing residues of apo wtSOD1 are shown: green, only missing in solution spectra (residues 44−46, 62, 65−68, 72−78, 81−82, 85−86, 118−119, 121−122); blue, only missing in solid-state spectra (residues 111, 128−131,143); orange, residues missing in both solution and solid-state spectra (residues 63−64, 69−71, 79−80, 83 and 120). Residues in apo wtSOD1 showing chemical shift differences between solution and microcrystals are shown as red spheres. The regions of the zinc and copper binding sites are highlighted by blue and gold spheres, respectively. The labeling has been reported only on one subunit of the SOD1 dimer for simplicity.

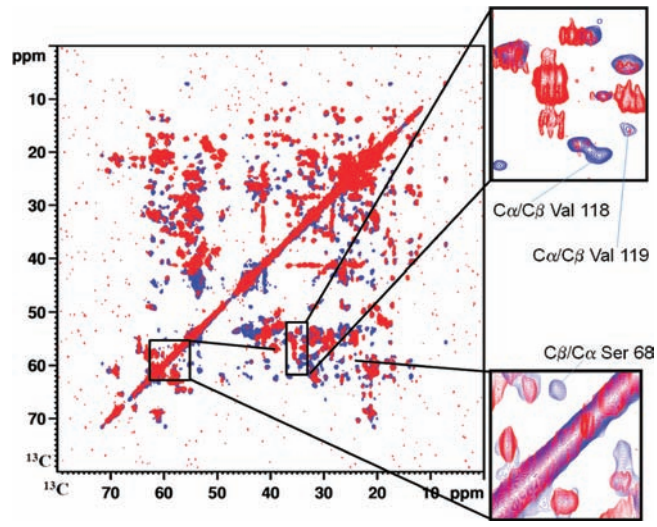

Figure 3. Overlay of the solid-state DARR spectrum (blue, 288 K) with the solution $^{13}C-^{13}C$ TOCSY spectrum (red, 288 K) of apo wtSOD1. In the inset two selected regions with residues visible only in the DARR spectrum but not in the $^{13}C-^{13}C$ TOCSY spectrum are shown.

analogous spectrum of the metalated form.[35] The ^{13}C assignment of the signals of the solid-state spectrum of apo wtSOD1 was carried out through recognition of spin systems and by directly comparing the DARR spectral pattern with the available aliphatic assignment on Cu,Zn ASSOD (AS stands for the more thermostable double mutant C6A and C111S) microcrystals.[35] Most cross-peaks in the DARR spectrum of apo wtSOD1 match very well those of the Cu,Zn ASSOD spectrum, and this allowed us to assign a large part of the cross-peaks present in the aliphatic region. Furthermore, overlapping peaks in the DARR spectrum, in particular the $^{13}C'-$aliphatic ^{13}C signals, can be resolved in 3D spectra, and therefore the DARR assignments were refined, expanded, and sequentially validated by combining NCA, NCO, NCACX, and NCOCX spectra. Moreover, the higher spectral resolution of apo ASSOD microcrystals helped us to further resolve several overlapped peaks in the spectra of apo wtSOD1. The chemical shifts of the backbone ^{15}N nuclei were also obtained.

Through this analysis we were able to assign all the signals present in the DARR spectrum. Around 83% of the backbone nuclei (80% C′, 82% N, and 87% Cα) and 82% of the non aromatic side-chain ^{13}C nuclei were assigned for apo wtSOD in microcrystals (Table S1). The 15 residues that escaped detection in the DARR spectrum are located in loops IV (63−64, 69−71, 79−80, 83), VI (111), and VII (129−131, 133, and 143) and in strand β6 (120) (orange and blue regions in Figure 2). It is to be noted that one dimer of the asymmetric unit of the X-ray structure of the apo wtSOD1 shows clear breaks in the electron density in the same loop regions.[19] This can be due to static disorder or residual conformational dynamics. Thus, even in the crystal lattice environment, these portions of the protein remain remarkably floppy at room temperature.

The spectral assignment in solution for apo wtSOD1, which had already been largely available (72% for Cα nuclei),[19] was here expanded by integrating the information from solid-state $^{13}C-^{13}C$ DARR and solution $^{13}C-^{13}C$ TOCSY spectra. Many parts of these two spectra are indeed superimposable (Figure 3). By plotting the more extensive solid-state assignment onto the $^{13}C-^{13}C$ TOCSY spectrum, the solution assignment was expanded in the β-strands 5 and 7 and in the loop between β-strands 6 and 7 (loop VI, residues 104−106). All the resolved signals present in the solution spectra of apo wtSOD1 were assigned. The assignment of Cα nuclei in the apo wtSOD1 in solution now reaches 77% (seven additional Cα assigned). The residues whose resonances are missing in solution are in loop IV and in the second β-sheet, formed by strands β4, β5, β7, and β8 (Figure 2). Many of the corresponding signals that are observed in the solid state are in well-resolved regions of the spectrum (Figure 3 insets), and therefore their undetectability in solution indicates that they are either broadened or moved into the crowded spectral region typical of unstructured residues. The whole second β-sheet is well formed in the solid, but part of it appears to be very conformationally disordered in solution. The same structural features in solution, including a less organized second β-sheet, have been observed also for the monomeric apoSOD1 species obtained through mutations at the subunit interface (M2 ASSOD1),[34] which has solution NMR spectra essentially superimposable to those of dimeric apo SOD1 except at the dimer interface and around the two point mutations C6A and C111S. However, the sharper signals arising from the halved molecular weight and the higher solubility produce higher quality spectra than those of dimeric apo wtSOD1, permitting the signals corresponding to the 62−83 (loop IV) stretch to be visible and assigned in this species.[34] All of them are in the crowded region typical of unstructured residues,[34] accounting for their undetectability in the dimeric form.

When all available spectra of apo and metalated wtSOD1 are compared with one another,[35−38] it appears that the apo SOD1 forms in solution differ significantly from any other form or state, including the apo wtSOD1 in microcrystals. In

(35) Pintacuda, G.; Giraud, N.; Pierattelli, R.; Böckmann, A.; Bertini, I.; Emsley, L. *Angew. Chem. Int. Ed.* **2007**, *46*, 1079–1082.
(36) Banci, L.; Bertini, I.; Cramaro, F.; Del Conte, R.; Viezzoli, M. S. *Eur. J. Biochem.* **2002**, *269*, 1905–1915.
(37) Banci, L.; Benedetto, M.; Bertini, I.; Del Conte, R.; Piccioli, M.; Viezzoli, M. S. *Biochemistry* **1998**, *37*, 11780–11791.
(38) Banci, L.; Bertini, I.; Cantini, F.; D'Amelio, N.; Gaggelli, E. *J. Biol. Chem.* **2006**, *281*, 2333–2337.

Table 1. TALOS+ Predictions of the Ramachandran Regions Based on Chemical Shifts of Cα, C′, and N Nuclei of apo wtSOD1 in Microcrystals (ApoWTSOD1 SS), apo wtSOD1 in Solution (ApoWTSOD1 Sol), and apo M2 ASSOD in Solution (ApoM2ASSOD1 Sol)[a]

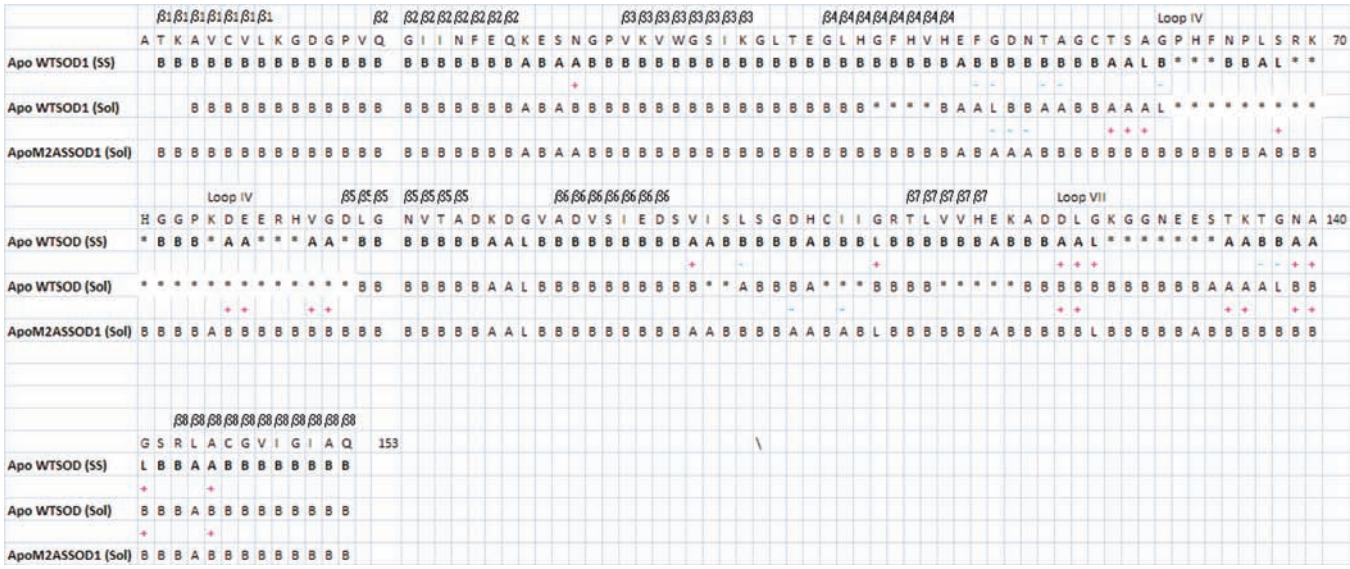

[a] Plus (+) indicates a change from A (or L) to B region on passing from apo wtSOD1 in microcrystals (bold) to apo wtSOD1 or apo M2 ASSOD in solution, while minus (−) indicates a change from B to A (or L) region.

particular, the spectra of the latter are much closer to those of the metalated Cu,Zn SOD1 form (both in solution and in the solid state) than to those of the solution apo forms.

The residues that experience the most significant changes in chemical shift between the solution and the solid state of the apo forms are located in loops IV (as seen from M2-ASSOD1) and VII (as seen from both M2 ASSOD1 and wtSOD1) (Figure 2). In particular, the largest chemical shift differences are observed for Asn65, Val81, and Gly82 and for residues 135−140 (red spheres in Figure 2). Val81 and Gly82 (loop IV) are in between two of the zinc binding residues (His80 and Asp83), while the stretch 135−140 (loop VII) is located in a region close to the zinc binding site. Residue Asn 65 is spatially close to Val81 and Gly82 (Figure 2).

The comparison between the chemical shifts of the flexible species in solution and those of the microcrystalline state highlights interesting features of the solution state. Indeed, chemical shift differences, although they are qualitative in nature, are sensitive reporters of local structural changes, which can thus be revealed also for a state, such as the solution state, characterized by conformational disorder. Thanks to the availability of the crystal state of both the 3D structure and the chemical shifts, the latter can be compared with the solution chemical shifts, thus obtaining information on which residues may undergo changes in conformation on passing from the crystal to the solution. It should be stressed that not the chemical shifts, as such, but their differences for forms of the same protein in different states are taken as indicators of conformational changes.

The NMR behavior of apo SOD1 indicates that the lack of metal ions together with the free environment of the solution state relax the structure of the apo form, which may thus take a conformation more prone to oligomerize. From the pattern of chemical shift changes, the primary structural rearrangement of the SOD1 β-barrel in the absence of metal ions toward an aggregation-prone form points to an initial disrupting of loops IV and VII.

Over 100 mutations in SOD1 have been linked to familial amyotrophic lateral sclerosis (http://alsod.iop.kcl.ac.uk/index.aspx). These mutations are predominantly single amino acid substitutions, although deletions, insertions, and C-terminal truncations also occur.[7] Despite the extensive studies on ALS-related mutants, a common link between them and SOD1 aggregation is not clear yet. Indeed, these mutations are spread throughout the whole SOD1 sequence (with the exception of strand β3) and have various types (e.g., protein stability, metal affinity, net charge, and susceptibility to disulfide reduction) and levels (more or less marked) of influence on the structure and properties of SOD1.[23,39−41] This makes it very difficult to correlate the nature of the mutation with their potential effects on the regions (loops IV and VII) that we have identified as relevant for initiating SOD1 fibrillation. Moreover, the latter regions do not carry a higher density of ALS-related mutations than other protein regions.

A closer inspection of the chemical shift differences between the solid-state and solution NMR spectra of apo SOD1 shows that for several residues, most of which are in loops IV and VII, the changes are so marked as to cause a change in the Ramachandran region of the residue itself (Table 1), as predicted by the TALOS+ program[33] (while fewer residues change Ramachandran region on passing from the metalated state to the apo form in the solid state; see Table S2). Remarkably, in the majority of such cases, the change from the solid state to the solution state of the apo form involves a transition from the A (or L) region to the B region. [The A,B notation rather than α,β is used here because isolated residues in A or B regions do not necessarily belong to α-helix or β-strand elements of secondary structure.] This behavior indicates an increase in β-propensity for several residues in the second half of loop IV and at the beginning and at the end of loop VII on passing from solid state to solution, which is also consistent with the observation of an increase in the total amount of β-structures as judged from CD spectra in solution compared to the β-content of the X-ray structure of the apo form.[6] Furthermore, residue

(39) Lindberg, M. J.; Bystrom, R.; Boknas, N.; Andersen, P. M.; Oliveberg, M. *Proc. Natl. Acad. Sci. U. S. A.* **2005**, *102*, 9754–9759.
(40) Tiwari, A.; Hayward, L. J. *J. Biol. Chem.* **2003**, *278*, 5984–5992.
(41) Nordlund, A.; Oliveberg, M. *HFSP J.* **2008**, *2*, 354–364.

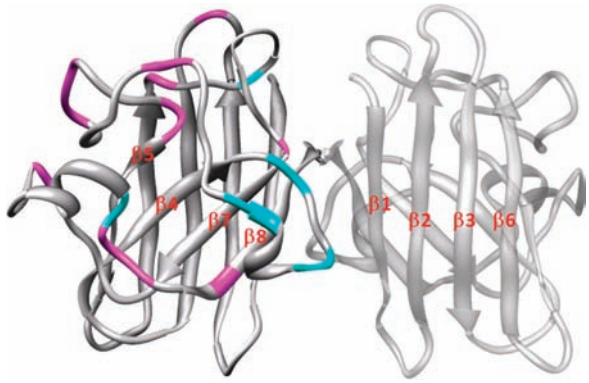

Figure 4. Mapping of the residues showing propensity to change from the A (or L) region of the Ramachandran plot to the B region (magenta) and from the B region to the A (or L) region (blue) on passing from apo solid state to apo solution state.

145, which is in the middle of β-strand 8 but is anomalously in the A region in the solid-state apo form, reverts to the B region in solution. In a few cases the opposite change is observed; that is, a few residues in the beginning of loop IV and in the middle of loop VII show an increased α-propensity. The changes are graphically summarized in Figure 4. The emerging picture is that the loops connecting the β-strands 4−5 (loop IV) and 7−8 (loop VII), having a large tendency to be unstructured in the apo state in solution, could be responsible for transiently forming additional stretches of β-strands that may drive the fibril formation process.

The availability of the chemical shift values of the apo form in the solid state has been crucial for shedding light on the possible initial steps of SOD1 fibrillation. In fact, the sizable differences in chemical shifts between the metalated and apo forms in solution, together with the absence of signals from several residues in the apo state, could have suggested that the apo state has an intrinsically different structure with a relatively high disorder. However, the apo form in the solid state is very similar to the metalated one, even in the absence of the intramolecular disulfide bridge, which causes only local differences.[17] Since crystallization of the apo form "traps" a structure that is likely to be present in solution at a non-negligible amount, we can conclude that the "metalated-like" structure of apo SOD1 exists in solution. Therefore, the observed NMR parameters for the apo form in solution represent a dynamic average of this form with another form (or forms) that is even more distant from the "metalated-like" conformation than can be guessed from the solution data. It would be reasonable to speculate that the stretches of residues whose signals are missing in solution are actually undergoing an equilibrium between the well-folded, dimeric, "metalated-like" species and a species where a few nascent β-strands may even begin to form the intermolecular interactions that start the oligomerization process. Table 1 indicates that possible candidates are residues 62−83 and 121−141.

This information has a strategic relevance for understanding the interactions and the mechanisms leading to SOD1 fibril formation.

Acknowledgment. Financial support from INSTRUCT Contract no. 211252 " Integrated Structural Biology Infrastructure", CERM PRIN 2007-2007M5MWM9 "Gli ioni metallici nelle interazioni proteina-proteina", and the European Commission (Project SPINE2-COMPLEXES-No. 031220) is gratefully acknowledged.

Supporting Information Available: We report the technical description of the solid-state NMR experiments, the assigned ^{15}N and ^{13}C resonances of apo wtSOD1 microcrystals, and the comparison between TALOS+ predictions of secondary structures based on chemical shifts of Cα, C$'$, and N nuclei. This material is available free of charge via the Internet at http://pubs.acs.org.

JA1069689